Design of an Energy-efficient Hybrid UWB-RF Indoor Distance Estimation System

Sabrine Khriji[a], Dhouha El Houssaini[b] and Olfa Kanoun[c]
Chair of Measurement and Sensor Technology, Chemnitz University of Technhology, Reichenhainer Straße 70, 09126 Chemnitz, Germany

Keywords: WSN, UWB, RF, Indoor Localization, Energy-saving, Wireless Communication.

Abstract: Wireless Sensor Network (WSN) plays a significant role in modern applications by offering different services, including state machines monitoring, predictive maintenance, and vehicle/store tracking. In such applications, it is crucial to apply localization methods to identify the current location of sensor nodes with high accuracy. Due to the energy constraint of sensor nodes, the energy consumption needs to be highly considered while performing the localization process. In this regard, this paper aims to design an energy-efficient and accurate localization system. Therefore, a novel hybrid solution is designed involving the Ultra Wide Band (UWB) technology and Radio Frequency (RF) transceiver. The UWB is based on Decawave's DWM1000 transceiver, which provides accurate distance measurements with a high power consumption. To reduce the power consumption, the data transmission between nodes is performed by the low-power RF transceiver. Using this architecture, the experimental validation shows a good performance in both power consumption and accuracy. The system's overall power consumption is reduced as well as a 10-centimeter accuracy level is achieved.

1 INTRODUCTION

Internet of Things (IoT) is nowadays of high interest in several sectors, including smart home, precision agriculture and e-health and industry 4.0 (Kanoun et al., 2021). In particular, Wireless Sensor Networks (WSNs) are gaining importance as enabling technology for monitoring and decision-making (Khriji et al., 2018), (El Houssaini et al., 2018a). With the advancements in WSNs, indoor localization becomes inevitable to track objects in indoor environments by offering many services, including predictive maintenance, store tracking and state machine monitoring (Höflinger et al., 2018), (Obeidat et al., 2021) and (El Houssaini et al., 2018b). Therefore, different positioning techniques are investigated to locate wireless sensor nodes.

Determining the current location of sensor nodes with high accuracy is the principal target of most existing localization studies. However, this requires a high power demand. Due to the energy constraint of sensor nodes, the energy consumption needs to be highly considered while performing the localization process. Only a few research (Kaur and Malhotra, 2016), (Cheng, 2021), and (Amutha et al., 2020) address the energy aspects of localization along with the accuracy. Therefore, the main aim of this paper is to establish a trade-off between accuracy and energy consumption for indoor positioning. In this context, an energy-efficient accurate positioning system is designed, which embeds the Ultra Wide Band (UWB) compliant wireless transceiver module, DWM1000 and the low-power wireless module, panStamp. The first module determines the distance between nodes with high accuracy. The distance calculation as well as performing different packets transmission/reception are carried out with the low-power radio transceiver in-built on the panStamp node. Thus, it reduces the overall power consumption needed for node positioning. To conclude, the key contributions of this work are:

- A panoramic view of indoor positioning technologies
- Design of energy-efficient accurate positioning system involving UWB wireless module and low-power RF transceiver

The rest of the paper is organized as follows. Section

[a] https://orcid.org/0000-0002-0562-0116
[b] https://orcid.org/0000-0003-1764-6601
[c] https://orcid.org/0000-0002-7166-1266

Khriji, S., El Houssaini, D. and Kanoun, O.
Design of an Energy-efficient Hybrid UWB-RF Indoor Distance Estimation System.
DOI: 10.5220/0011012700003118
In *Proceedings of the 11th International Conference on Sensor Networks (SENSORNETS 2022)*, pages 249-255
ISBN: 978-989-758-551-7; ISSN: 2184-4380

2 presents an overview of indoor positioning technologies with highlighting the use of the UWB technology. The design and implementation of the proposed distance measurement architecture is provided in section 3. Section 4 presents the experimental results of the designed system in terms of accuracy and power consumption. Section 5 concludes the paper.

2 OVERVIEW OF INDOOR POSITIONING TECHNOLOGIES

Indoor positioning can be divided into building dependent and building independent (Alarifi et al., 2016) technologies (see Fig. 1). Building dependent technologies rely on the building, where they are going to be installed. They are based on an available technology in the building, or on the building's structure and layout. This category can be further classified into two classes: Dedicated infrastructure required and building's infrastructure utilized. The indoor positioning that needs a dedicated infrastructure can be RFID, infrared, ultrasonic, Zigbee and UWB.

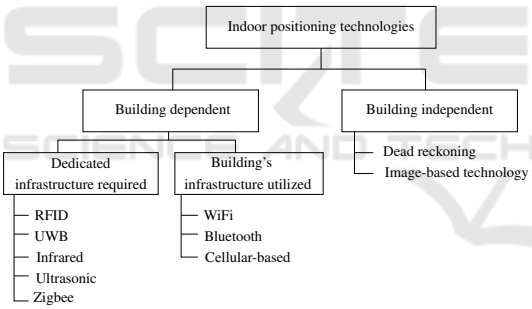

Figure 1: Indoor positioning technologies.

RFID systems rely on proximity detection, and hence have an accuracy of dm-m level (Xu et al., 2017). A larger area requires several RFID tags, resulting on increasing the cost as well as power consumption. UWB systems can work in Non-Line of Sight (NLOS) conditions. UWB operates within 3.5 to 6.5 GHz, which does not interfere with other frequencies. The Infrared (IR) wireless communication uses the invisible spectrum of light (Arbula and Ljubic, 2020). Differential phase-shift and angle of arrival (AoA) localization methods are commonly used with IR technology. Another technology requiring the building's infrastructure is the ultrasonic technology. It is based on the ToF (Time of Flight) localization method. Therefore, ultrasound impulses are carried out by the tag to measure the distance to the anchor. This technology has a short-range, and does not interfere with electromagnetic waves.

The Zigbee technology can be also used to determine the nodes' positions. This technology is designed for applications requiring low throughput and low power consumption. It comprises a microcontroller and a multi-channel bidirectional radio on a single piece of silicon (Aykaç et al., 2017). Typically, Received Signal Strength (RSS) values have been employed to determine the distance between Zigbee-based sensor nodes.

WiFi, Bluetooth and cellular-based technologies refer to the indoor positioning technologies that use the building' infrastructure. WiFi positioning systems can reach up to a range of 50 m, but the accuracy obtained is very low (in meters).

Furthermore, building independent technologies can be a dead reckoning and image-based technologies. In dead reckoning, the current position of an object can be determined by its previous position, direction of travel and speed (Zhou et al., 2015). On the other hand, image-based technologies are often supported by cameras and computer vision technologies (Wu et al., 2018). A summary of different indoor positioning technologies is depicted in Table. 1.

Table 1: Indoor positioning technologies.

Technology	Range	Accuracy	Measuring Principle
RFID	50 m	dm-m	Cell of Origin
Ultra-Wide Band	50 m	cm	TWR,ToA,TDoA
Infrared	5 m	cm-m	Differential phase-shift, AoA
Ultrasound	10 m	cm	ToA, TDoA
Zigbee	20 -30 m	cm	Trilateration, RSSI
WiFi	50 m	m	RSSI,ToA,TDoA
Bluetooth	10 - 100 m	m	Proximity, RSS
Dead reckoning	-	m	Tracking
Cameras	10 m	mm-dm	Pattern recognition

3 DESIGNED HYBRID SYSTEM

The main aim of the proposed system is to determine the distance between sensor nodes with a high accuracy and less power consumption. The block diagram of the localization system architecture is depicted in Fig. 2.

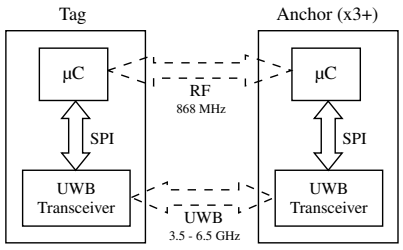

Figure 2: UWB localisation system architecture.

Therefore, the UWB system consists of a tag and

several anchors. Both tag and anchor consist of the same hardware, with a microcontroller and an UWB transceiver. The UWB technology is used to provide a high accuracy with limited range. A low-power microcontroller is connected to the UWB via Serial Peripheral Interface (SPI) to ensure the computation of distance measurements. A low-power radio transceiver with a frequency of 868 MHz is used to exchange other data needed by the application.

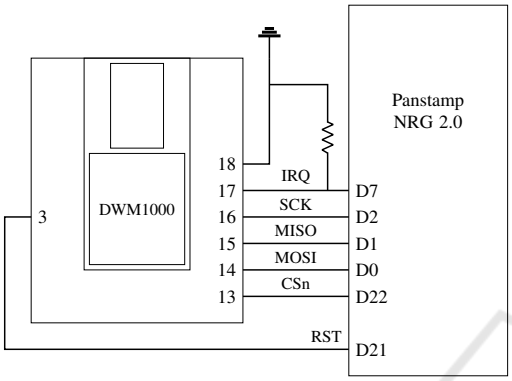

Figure 3: Interfacing DWM1000 with Panstamp NRG 2.0.

To determine the distance between the tag and anchor nodes, the wireless transceiver module DWM1000 is used, which is an IEEE802.15.4-2011 UWB compliant module. This transceiver is used only for communicating the distance between two nodes (DWM, 2021). The main advantage of the selected UWB transceiver is the high data rate communication, as it can transmit pulses with a bandwidth up to 6.8 Mbps. It determines also the positions of objects with an accuracy of 10 centimetres in NLoS conditions. It supports TDoA and ToF location techniques. This transceiver consists of the Two-Way Ranging (TWR) method, which determines the ToA of the UWB RF signal. Then, it calculates the distance between nodes by multiplying the time by the speed of light.

To measure the distance between two nodes, three messages need to be exchanged (see Fig. 4). The tag sends a *Poll* message to know the address of the anchor in time referred to Time of Sending Poll (T_{SP}). The time of the *Poll* reception (T_{RP}) is recorded by the anchor, which replies with the response message at time T_{SR}. By receiving the response message, the tag node records the time T_{RR}, and composes a *Final* message, including its address, T_{SP}, T_{RR} and T_{SF} information. Based on the timestamps, the communicated signals between the tag and anchor are used to measure the ToA of the UWB signal, as presented in equation 1. Thereby, the distance is determined by multiplying the ToA of the UWB signal with the speed of light c as depicted in equation 2.

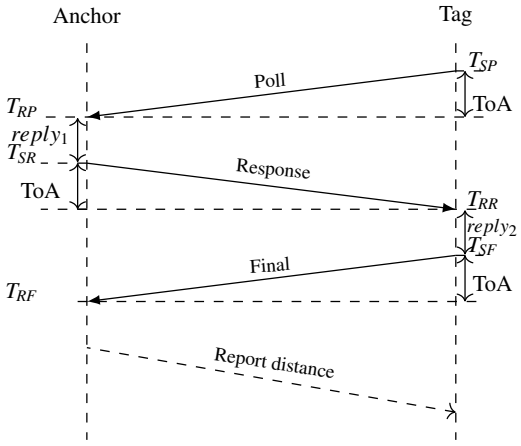

Figure 4: Distance measurement using TWR technique implemented on DWM1000 transceiver.

$$ToA = \frac{(T_{RR}-T_{SP})-(T_{SR}-T_{RP})+(T_{RF}-T_{SR})-(T_{SF}-T_{RR})}{4} \quad (1)$$

$$distance = c \times ToA \quad (2)$$

Due to limited ressources of sensor node, the power consumption is a key feature in wireless sensor networks. Thereby, choosing low-power hardware can reduce the overall node power consumption. In this direction, the low-power RF-based wireless sensor node, panStamp, is used. The module is based on the CC430F5137 System on chip (SoC), including the MSP430 microcontroller and CC1101 radio chip (Salem et al., 2019), which operates at different frequencies like 433 MHz, 868 MHz and 915 MHz. It supports SPI communication, which enables the communication with the DWM1000 module. The connections are shown in Fig. 3. The panStamp communicates with the DWM1000 at 4 MHz SPI frequency. Apart from SPI connection, a reset line (RST) and interrupt request (IRQ) lines are connected to the DWM1000. The RST line can be pulled low to reset the DWM1000 module. The IRQ is an input to the Panstamp and is active high. An interrupt is generated by the DWM1000 to notify Panstamp at each event such as transmission, reception or wake up.

Fig. 5 shows the block diagram of the tag node. The initialization step includes the configuration of the SPI interface with the microcontroller. The SPI communication is initiated at the desired rate. During this phase, the DWM1000 transmission rate and frequency are configured. A TimerDelay is set, which defines the rate of the distance measurement. Every time, the internal clock of the microcontroller reaches the TimerDelay, a ranging cycle is initiated. This

starts with a polling message sent by the tag, and ends after receiving the range report from the anchor. The tag is responsible for sending timestamps in the range message. After each range measurement, the tag switches to the sleep mode and wakes up again before initiating the measurement sequence.

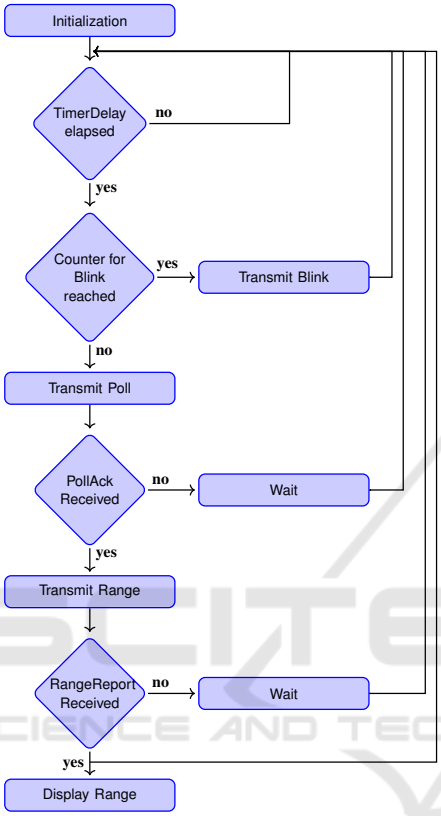

Figure 5: Ranging algorithm for the tag node.

As depicted in Fig. 6, the anchor node starts in the receiving mode, waiting for a Poll message from the tag. On receiving this message, it acknowledges by transmitting a PollAck message and waits for a range message. The range message includes all the timestamps calculated on the tag side and, along with the timestamps measured at the anchor, a Time-of-Flight (ToF) is computed. This ToF is converted into the distance, and thus transmitted back to the tag as a range report message.

4 EXPERIMENTAL RESULTS

The designed indoor localization system is evaluated in terms od power consumption and accuracy.

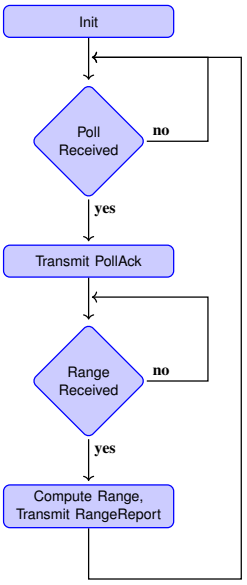

Figure 6: Ranging algorithm for the anchor node.

4.1 Power Consumption

The main aim of using a panStamp as a microcontroller for DWM1000 is its low-power consumption along with its wireless capabilities. The Rx and Tx current for panStamp is 18 mA and 36 mA respectively, which is far less than the DWM1000 current consumption (140 mA and 160 mA). Thus, messages that do not play a part in the range calculation can be transmitted using the radio module in panstamp instead of DWM1000. Messages that can be replaced are Blink, RangingInit, RangeReport.

Since receiving a message consumes a lot of power, we turn on the receiver exactly at the time a message is expected. Thus, scheduling of the messages is very important. Also, when in sleep mode, the microcontrollers of tag and anchors need to communicate with each others to wake up the DWM1000 at the right time. In the case of panStamp, this is carried out using the radio module available on panStamp. The maximum current consumption as per the datasheets of DWM1000 and panStamp is given in Table 2. Based on the timestamps generated from Panstamp using the serial monitor, the total current consumption of the system can be estimated accordingly as the maximum current consumption is known. For this, consider a measurement cycle between a Tag and Anchor. As the radio signals travel at the speed of light, the signal transmission time in the air is very low and would not differ much for the operating range of 50 meters. Various events are recorded using the serial monitor of the Panstamp and a summary of time and current required for each event in tag and anchor

can be seen in Fig. 3, Fig. 8 and Tables 3 and 4.

Table 2: Maximum current consumption for DWM1000 and panStamp.

Device Mode	DWM1000	Panstamp
Tx	140 mA	18 mA
Rx	160 mA	36 mA
Deepsleep	200 nA	2 uA
Idle	13.4 mA	2 mA

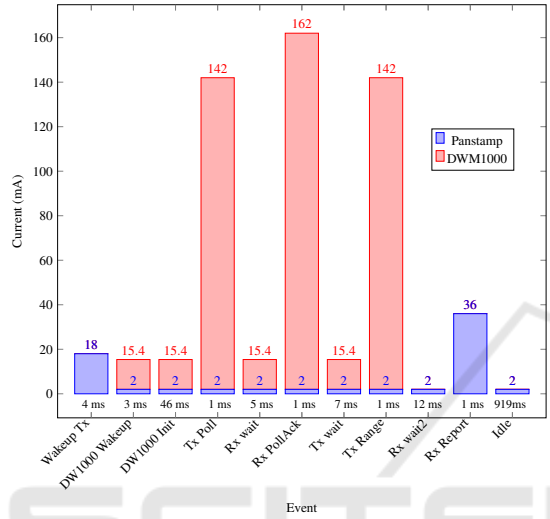

Figure 7: Interfacing DWM1000 with Panstamp NRG 2.0.

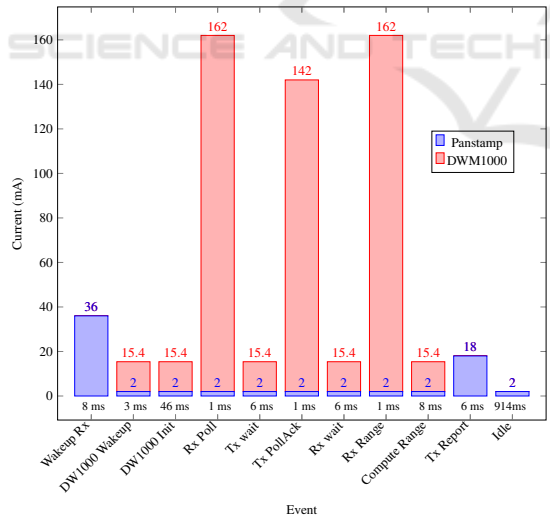

Figure 8: Estimated current consumption in anchor for one cycle.

Each cycle includes a range measurement between a Tag and Anchor using DWM1000 and panStamp. Initially, both DWM1000 modules are in deep sleep mode and the panStamp node of the tag is in Idle mode, while the panStamp node of the anchor is in receiving mode. Therefore, the total current consumption is 2 mA for the tag, and 36 mA for the anchor node. To initiate a measurement, the tag sends a wake-up signal to the anchor via the radio module of panStamp. This message includes 2 bytes signal with the address of the anchor node and message ID for wake-up command. Immediately, after the transmission from the tag, the radio module of panStamp is turned off and an SPI signal from panStamp wakes up the DWM1000. This takes approximately 3 ms. As the DWM1000 is in deep sleep mode, it needs to be reconfigured. The initialization of the module takes around 46 ms. The DWM1000 starts in idle mode and consumes around 13.4 mA current.

Table 3: Estimated current consumption of the tag for one cycle.

Event	panStamp		DWM1000		Time (ms)	Total Current (mA)
	State	Current (mA)	State	Current (mA)		
Wakeup Tx	Tx	18	Deepsleep	0.0002	4	18.0002
DW1000 wakeup	Idle	2	Idle	13.4	3	15.4
DW1000 init	Idle	2	Idle	13.4	46	15.4
Tx Poll	Idle	2	Tx	140	1	142
Rx wait	Idle	2	Idle	13.4	5	15.4
Rx PollAck	Idle	2	Rx	160	1	162
Tx wait	Idle	2	Idle	13.4	7	15.4
Tx range	Idle	2	Tx	140	1	142
PS Rx wait	Idle	2	Deepsleep	0.0002	12	2.0002
Rx RangeReport	Rx	36	Deepsleep	0.0002	1	36.0002
Idle	Idle	2	Deepsleep	0.0002	919	2.0002

On receiving the wake-up command from the radio module of panStamp, the anchor node wakes up the DWM1000 module via the SPI communication. The receiver of the panStamp radio is also turned off to save power. After completing the initialization of the DWM1000, the receiver is turned on, and the tag transmits the first message from DWM1000, the Poll message. Thus, the anchor receives this message at the same time. The time difference between turning on the receiver and actual reception is calculated at the anchor side, which is approximately 1 ms. Therefore, the 160 mA consumption of the DWM1000 in the receiving state only occurred for 1 ms. The transmission of 128 symbol preamble and 20 bytes of data requires only 0.2 ms when operating at 6.8 Mbps data rate. This means that the transmitter of the DWM1000 would be operating only for 0.2 ms consuming 140 mA current. All the transmissions in the DWM1000 are carried out at this rate, but for calculating the current consumption, we assume the transmission time as 1 ms for all the messages.

The DWM1000 is a half-duplex transceiver that can either transmit or receive a message at a single time. By default, the module switches to its idle state after transmitting or receiving a message. After receiving the Poll message, the anchor saves the timestamp in the panStamp memory, and starts transmitting the PollAck message. This time is termed as Tx wait, where the DWM1000 is in idle state and ready for

Table 4: Estimated current consumption of the anchor for one cycle.

Event	Panstamp		DWM1000		Time (ms)	Total Current (mA)
	State	Current (mA)	State	Current (mA)		
Wakeup on Rx	Rx	36	Deepsleep	0.0002	8	36.0002
DW1000 wakeup	Idle	2	Idle	13.4	3	15.4
DW1000 init	Idle	2	Idle	13.4	46	15.4
Rx Poll	Idle	2	Rx	160	1	162
Tx wait	Idle	2	Idle	13.4	6	15.4
Tx PollAck	Idle	2	Tx	140	1	142
Rx wait	Idle	2	Idle	13.4	6	15.4
Rx range	Idle	2	Rx	160	1	162
Compute range	Idle	2	Idle	13.4	8	15.4
Tx RangeReport	Tx	18	Deepsleep	0.0002	6	18.0002
Idle	Idle	2	Deepsleep	0.0002	914	2.0002

its next transmission. The tag also saves the timestamp it sent the Poll message and is now waiting for its next reception. Since the PollAck is not sent immediately, the tag stays in idle state to save power, which is termed as Rx wait. After waiting for a few seconds, the tag switches to receiving mode to receive the PollAck message. Higher Rx wait time refers to a lower reception time for the tag resulting on power saving. The Rx wait time is gradually increased in the tag until the message reception is possible. Once stable receptions are available, the time is fixed as Rx wait time.

Upon receiving the PollAck, the tag records this timestamp. This timestamps has to be transmitted to the anchor. During the Tx wait, the tag gathers all the available timestamps and prepares the ranging message. This took around 7 ms for the tag. Once the message is ready, the tag transmits this range message and sets the DWM1000 to deep sleep. The Rx wait time for this message was also optimized on the anchor side, where the DWM1000 was idle for 6 ms. On receiving the range message, the anchor has to calculate the exact range between the tag and anchor based on the timestamps available and those received from the range message. This calculation took around 8 ms after which the DWWM1000 is switched from idle state to deep sleep mode. Since the range is already calculated, both the DWM1000 are not required to be active and are sent to deep sleep. At this point, only the anchor knows the range between the two points, and has to transmit this information to the tag. The transmission of the RangeReport happens over the panStamp radio module. To receive this message, the panStamp receiver at the tag has to be turned on as well. The Rx wait time is calculated and upon receiving the RangeReport message, the Panstamp Radio module is turned off. At this point, both the tag and anchor have calculated the range, and enter the idle state, waiting for the next measurement cycle. The next measurement cycle starts with the wake-up signal from the tag, but to receive this message the panStamp radio has to be in the receiving mode. Therefore, depending upon the update rate required, the receiver at the anchor is automatically turned on after a fixed delay time. The panStamp can also be used in Wake-on-Radio (WOR) mode to continuously check for the reception after certain time intervals.

By combining the total estimated current consumption with the time required for each state, an average current consumption can be calculated. For ranging a new measurement every second, the average current consumption estimated is 3.35 mA for tag and 3.75 mA for anchor. This is a considerable reduction in the power consumption for DWM1000 modules along with the microcontroller. Reducing the update rate would further reduce power consumption.

4.2 Distance Measurements

Fig. 9 shows the distance measurement using DWM1000 interfaced with a panStamp module.

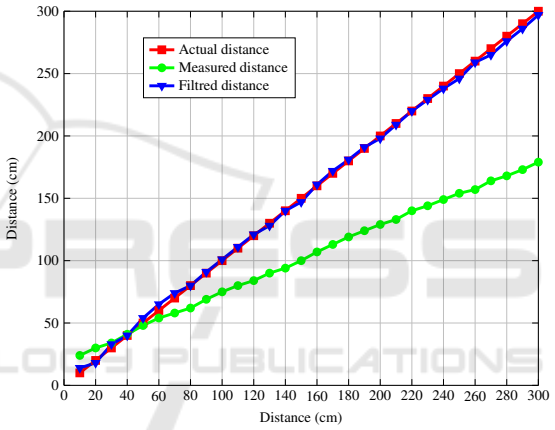

Figure 9: Measured distance using DWM1000 with Panstamp.

It can be seen that the raw measured distance is far away from the actual distance, but follows a linear pattern. This can be corrected by adjusting the antenna delay value provided in the timestamp calculation. The antenna itself has a fixed transmission delay. To compensate for this delay in DWM1000, an integer value is set during the initialization. Since the plot is linear for the raw measured data, a linear filter is applied during the calculation of the distance to get more accurate readings. Using least squares fitting, the following polynomial is obtained for the curve:

$$Filterdist = 0.53375 \times Measurdist + 20.469 \quad (3)$$

The raw measurements are then linearised using this filter. It can be seen from Fig. 9 that an accuracy of 10 cm can be achieved in indoor environment using a DWM1000 with panStamp.

5 CONCLUSION

An Ultra-wideband localization system is designed using Decawave's DWM1000 and panStamp wireless node. The panStamp enables a second channel for the communication within the nodes, thus keeping the UWB messages to the minimum. Two frequency bands are utilized by the system, 6.5 GHz for DWM1000 and 868 MHz for the panStamp radio. The Panstamp operates at very low current, which reduces the overall current consumption of the system. It is estimated that the system consumes a total of 3.35 mA current for tag and 3.75 mA current for anchor during operation at 1 Hz update frequency. Even with the low power microcontroller, a good performance of the system is achieved. Tests performed indoors within a distance of 3 meters show an accuracy of 10 cm.

REFERENCES

(2021). *DW1000 Datasheet*. decaWave.

Alarifi, A., Al-Salman, A., Alsaleh, M., Alnafessah, A., Al-Hadhrami, S., Al-Ammar, M. A., and Al-Khalifa, H. S. (2016). Ultra wideband indoor positioning technologies: Analysis and recent advances. *Sensors*, 16(5):707.

Amutha, J., Sharma, S., and Nagar, J. (2020). Wsn strategies based on sensors, deployment, sensing models, coverage and energy efficiency: Review, approaches and open issues. *Wireless Personal Communications*, 111(2):1089–1115.

Arbula, D. and Ljubic, S. (2020). Indoor localization based on infrared angle of arrival sensor network. *Sensors*, 20(21):6278.

Aykaç, M., Erçelebi, E., and Aldin, N. B. (2017). Zigbee-based indoor localization system with the personal dynamic positioning method and modified particle filter estimation. *Analog Integrated Circuits and Signal Processing*, 92(2):263–279.

Cheng, Q. (2021). A robust indoor localization algorithm for wsn in los and nlos environment. In *2021 IEEE 11th International Conference on Electronics Information and Emergency Communication (ICEIEC) 2021 IEEE 11th International Conference on Electronics Information and Emergency Communication (ICEIEC)*, pages 91–94. IEEE.

El Houssaini, D., Khriji, S., Besbes, K., and Kanoun, O. (2018a). Wireless sensor networks in agricultural applications. In *Energy Harvesting for Wireless Sensor Networks*, pages 323–342. De Gruyter Oldenbourg.

El Houssaini, D., Mohamed, Z., Khriji, S., Besbes, K., and Kanoun, O. (2018b). A filtered rssi model based on hardware characteristic for localization algorithm in wireless sensor networks. In *2018 32nd International Conference on Advanced Information Networking and Applications Workshops (WAINA)*, pages 118–123. IEEE.

Höflinger, F., Bordoy, J., Zhang, R., Bannoura, A., Simon, N., Reindl, L. M., and Schindelhauer, C. (2018). Localization system based on ultra low-power radio landmarks. In *SENSORNETS*, pages 51–59.

Kanoun, O., Khriji, S., Naifar, S., Bradai, S., Bouattour, G., Bouhamed, A., El Houssaini, D., and Viehweger, C. (2021). Prospects of wireless energy-aware sensors for smart factories in the industry 4.0 era. *Electronics*, 10(23):2929.

Kaur, R. and Malhotra, J. (2016). Efficient localization in wsn based on structured deployment of anchor nodes in dv-hop. *International Journal of Future Generation Communication and Networking*, 9(3):155–166.

Khriji, S., El Houssaini, D., Kammoun, I., and Kanoun, O. (2018). A fuzzy based energy aware unequal clustering for wireless sensor networks. In *International Conference on Ad-Hoc Networks and Wireless*, pages 126–131. Springer.

Obeidat, H., Shuaieb, W., Obeidat, O., and Abd-Alhameed, R. (2021). A review of indoor localization techniques and wireless technologies. *Wireless Personal Communications*, pages 1–39.

Salem, J. B., Khriji, S., Baklouti, M., Kammoun, I., and Kanoun, O. (2019). Testbed implementation of a fuzzy based energy efficient clustering algorithm for wireless sensor networks. In *2019 16th International Multi-Conference on Systems, Signals & Devices (SSD)*, pages 351–356. IEEE.

Wu, Y., Tang, F., and Li, H. (2018). Image-based camera localization: an overview. *Visual Computing for Industry, Biomedicine, and Art*, 1(1):1–13.

Xu, H., Ding, Y., Li, P., Wang, R., and Li, Y. (2017). An rfid indoor positioning algorithm based on bayesian probability and k-nearest neighbor. *Sensors*, 17(8):1806.

Zhou, Z., Chen, T., and Xu, L. (2015). An improved dead reckoning algorithm for indoor positioning based on inertial sensors. In *International Conference of Electrical, Automation and Mechanical Engineering (EAME 2015)*, pages 369–371.